A USER-FRIENDLY TOOL FOR SIMULATING THE TIME-DEPENDENT FIELD DISTRIBUTION IN PE INSULATION ON THE BASIS OF A PHYSICAL APPROACH

Séverine LE ROY, Laboratoire Plasma et Conversion d'Energie, (France), severine.leroy@laplace.univ-tlse.fr
Fakher BOUFAYED, Laboratoire Plasma et Conversion d'Energie, (France), fakherbo@yahoo.fr
Fulbert BAUDOIN, Laboratoire Plasma et Conversion d'Energie, (France), fulbert.baudoin@laplace.univ-tlse.fr
Gilbert TEYSSEDRE, Laboratoire Plasma et Conversion d'Energie, (France), gilbert.teyssedre@laplace.univ-tlse.fr
Christian LAURENT, Laboratoire Plasma et Conversion d'Energie, (France), christian.laurent@laplace.univ-tlse.fr

ABSTRACT

A bipolar model of transport intended to describe the behavior of polyethylene under DC stress has been recently developed. Though the model has not been pushed yet to the stage of using it routinely, it did lead to progress in the understanding of dielectric physics in the sense that various hypotheses for explaining a given experimental observation can be evaluated. The purpose of this communication is to give the general features of the model and to introduce the graphic interface allowing simulation in polyethylene plaques. Simulation has been developed with the purpose of giving outputs directly comparable with experimental data. The latter can be external current measurements or internal space charge distribution as obtained using the Pulsed Electro Acoustic technique. A demonstration of the software will be done at the conference. A comparison between simulation and experimental results is discussed in a companion paper.

KEYWORDS

Field distribution - Space charge - Graphic Interface - 1D modelling

INTRODUCTION

In recent years, a number of numerical models have been developed with the aim to reproduce the space charge behavior in organic insulators, mainly polyethylene, under DC or AC stress [1-5]. Among the driving forces for the development of these models we can name: the trends towards more compact systems in power engineering, leading to an increase in the power density - the trends towards higher reliability of electrical systems, due to their use in critical applications - the development of new materials for electrical application with tailored properties. Moreover, the increasing demand in solutions for predicting materials behaviour under stress is to be addressed on one hand with a better understanding of physical mechanisms underlying such behaviour, and on the other with disposable tools for modelling what such mechanisms imply as macroscopic properties and to confront such predictions with the actual behaviour of materials in systems. These general principles are tackled here with regard to internal field distortions due to charge generation and accumulation into polyethylene-based insulated high voltage DC cables submitted to thermoelectric stress. State of the art numeric techniques have been applied to resolve the transport equations in non stationary conditions, providing a prevision of the macroscopic behaviour in a reasonable computing time for DC stress conditions.

In this communication, we present the physical model and the software that has been developed for that purpose [6]. In the first part, we briefly present the general features of the physical model included in the software core coded in Fortran language. In the second part, we describe the graphic interface which has been developed under Java environment. This language has underlying advantages resorting to the open nature of the source (no issues with licence agreement) and to the large portability over different operating systems, requiring only recompilation under non-Windows OS. This would permit a large diffusion of such tool in a near future.

PHYSICAL MODEL

Figure 1 shows a schematic representation of system used for the simulations. The type of model is bi-polar, and features injection of electronic charges at both electrodes, charge trapping in traps distributed exponentially in trap depth, and hopping transport. For sake of simplification, recombination of charges and internal generation are not taken into account [5].
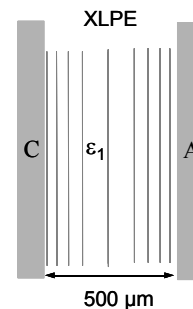

XLPE

C ε_1 A

500 µm

Figure 1: schematic representation of the one-dimensional system used for the simulation.

Trap distribution: The chemical structure of the material is taken into account by considering an exponential distribution of trap levels (Figure 2), i.e. a large amount of shallow traps corresponding to physical defects, and a smaller amount of deep traps corresponding to impurities. This exponential distribution of traps has a maximum limit in trap depth, and is of the form:

$$N_{t(e,h)} = N'_{(e,h)} \exp\left(\frac{-\Delta_{e,h}}{k_B T_{0(e,h)}}\right) \qquad \Delta_{e,h} \leq \Delta_{max(e,h)} \qquad (1)$$

where $N_{t(e,h)}$ is the trap density distribution, for electrons and

holes, and is characterized by the parameters N', T_0 and the maximum limit in trap depth Δ_{max}. This exponential distribution of trap levels holds for each kind of carrier (electrons and holes). Traps are considered to be filled from the deepest level upwards.
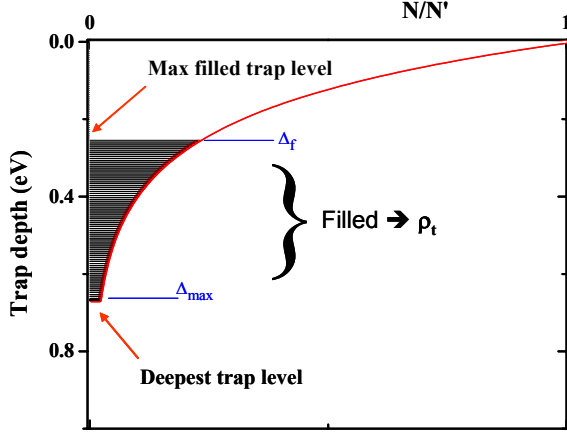

Figure 2: Distribution of trap levels for one kind of carriers. Δ_f defines here the upper filled level, which is variable as a function of time and space.

Mobility: Charge transport within insulating polymers is often described by a hopping mechanism in which carriers move from site to site by getting over a potential barrier. In our case the hopping charges essentially come from the highest filled trap state at a depth Δ_f, and the resulting mobility $\mu(x,t)$ is then function of the trapped charge density ρ_t (2):

$$\mu(x,t) = \frac{2.\upsilon.d}{E(x,t)} \left(\frac{\rho_t(x,t)}{N'k_B.T_0} + \exp\left(\frac{-\Delta_{max}}{k_B.T_0} \right) \right)^a \sinh\left(\frac{e.E(x,t).d}{2.k_B.T} \right) \quad (2)$$

with $a = \dfrac{T_0}{T} \rangle 1$ \quad (3)

and $d = \left(N'k_B T_0 \right)^{-\frac{1}{3}} \left(1 - \exp\left(-\frac{\Delta_{max}}{k_B T_0} \right) \right)^{-\frac{1}{3}}$ \quad (4)

where υ is the attempt to escape frequency, d is the average distance between traps, E(x,t) is the electric field, and e is the elementary charge.
If the electric field is small ($e.E.d \langle\langle k_B.T$), equation (2) can be reduced to:

$$\mu(x,t) = \frac{e.\upsilon.d^2}{k_B.T} \cdot \left(\frac{\rho_t(x,t)}{N'k_B.T_0} + \exp\left(\frac{-\Delta_{max}}{k_B.T_0} \right) \right)^a \quad (5)$$

When $T_0 \gg T$, only a fraction of charge ρ_f from the trapped charge ρ_t is available for conduction:

$$\rho_f(x,t) = \frac{\rho_t(x,t)}{1+a} \quad (6)$$

Generation of carriers: The only source of charge is the injection of electronic carriers at both electrodes. The injection for each kind of carrier follows a modified-Schottky law (7):

$$j_{e,h}(x,t) = A.T(x)^2 . \exp\left(-\frac{e.w_{e,h}}{k_B.T} \right) \left(\exp\left(\frac{e}{k_B.T} \sqrt{\frac{e.E(x,t)}{4.\pi.\varepsilon}} \right) - 1 \right) \quad (7)$$

where $j_h(x,t)$ and $j_e(x,t)$ are the injected fluxes of holes and

electrons at the anode and cathode respectively, A is the Richardson constant, w_e and w_h are the injection barriers. ε refers to the permittivity of the dielectric.
The time and space dependent equations describing the behaviour of charge carriers are the following, neglecting diffusion, and in Cartesian coordinates:

$$\frac{\partial n(x,t)}{\partial t} + \frac{\partial j(x,t)}{\partial r} = 0 \quad \text{continuity} \quad (8)$$

$$\frac{\partial E(x,t)}{\partial x} = \frac{\rho(x,t)}{\varepsilon} \quad \text{Poisson} \quad (9)$$

$$j(x,t) = \mu(x,t).\rho_f(x,t).E(x,t) \quad \text{transport} \quad (10)$$

NUMERICAL TECHNIQUES

The thickness d of the system is discretised using a non-uniform grid of elements of size Δx (typical order of magnitude being 0.4 µm for a 500 µm-thick sample), being tightened next to the electrodes, in order to follow the penetration of charge in the dielectric (See Figure 1). At each time of the simulation, the time step is calculated to be less than the quickest phenomenon occurring in the dielectric. It must also satisfy the Courant-Friedrichs-Lewy condition, for each mobile carrier. It means that the charge displacement within one time step (typical value of $\Delta t = 10^{-2}$ s) is less that the size of an element Δx.
The time and space dependent electric field and potential are calculated by discretization of the Poisson equation. The numerical method used to resolve steep front problems due to charge penetration in the dielectric is based on a scheme first developed by Leonard [7], avoiding numerical diffusion. To avoid production of negative densities of species, a flux limiter has been also included in the code. Further details on the numerical resolution of the equations in the model can be found in [8].

TREATMENT OF SIMULATION OUTPUTS

Results produced by the model cannot be directly compared to experimental data, especially space charge profiles obtained by the PEA method, for the following reasons. First, only internal charges are produced and not image charge on the electrodes. To account for image charges, surface charge densities have been added at the electrodes according to the following equation(s):

$$\rho_{cathode} = -\frac{1}{dx} \int_0^D \frac{(D-x)}{D} \rho(x,t)\partial x - \frac{\varepsilon V}{dx.D}$$

$$\rho_{anode} = -\frac{1}{dx} \int_0^D \frac{x}{D} \rho(x,t)\partial x - \frac{\varepsilon V}{dx.D}$$
\quad (11)

where *V* is the applied voltage and *dx* is the width of the cell on the electrode. Cathode is at abscissa 0.
Second, profiles obtained by the PEA method are, like with any other technique, accompanied by incertitude on the position of the charges. This results from a combination of the width of the excitation pulse, of the band pass of the piezoelectric sensor, of related amplification and of the oscilloscope (which also adds discretization), and of filtering of the signal during its processing. As a result, capacitive charges measured on a space-charge free material under voltage appear as Gaussian curves instead of a singled out point.

As it is not possible in practice to correct experimental data for incertitude associated to position of the charge, we have applied a numerical filter to our data in order to lose part of the resolution reached by the simulated profiles. This has been done by applying a Gaussian filter of the form:

$$g(x) = \exp\left[-a\left(x - \frac{nf}{2}\right)^2\right] \tag{12}$$

where a defines the width of the Gaussian (to be adapted to fit to measured profiles) and $nf/2$ is the centre of the Gaussian. The numerical filter is applied to both electrode and internal charges. Figure 3 shows an example of the spreading of the influence charge introduced by the filter in the case of capacitive charge (no internal charge and hence no image charge).
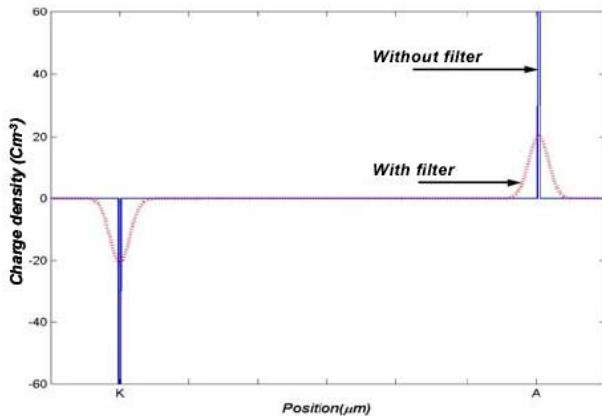

Figure 3: Introduction of capacitive charge on both electrodes (no charges in the bulk) and treatment by a Gaussian filter.

In order to use the software quite efficiently, a graphic interface has been developed. Its general features are given in the following part.

GRAPHIC INTERFACE

The program is constituted by the following files (size of 600kb in total) in a Java run-time environment:

o the Fortran-based executable code, referred to as Injection in the following;
o the Interface program which constitutes the user-friendly part of the package;
o an ASCII type file containing parameter model parameter values.

The Injection program

The Injection program calculates space charge density, current, electric field without recourse to the Interface itself. Parameters signification is self-explanatory as shown in Figure 4. The use of this program is limited to single dielectric of plaque geometry (an extension of the program has been developed for multiple-dielectric and co-axial geometry-see companion paper in this conference [9]) and only one polarization / depolarization cycle can be programmed, for adjustable times. An initial charge density for positive and negative carriers can be set, being homogeneous in the volume to simulate a charge distribution with zero net charge that cannot be measured using the space charge mapping techniques, or to take into account an initial distribution with non zero net charge, which could be the case for example when the density is below the sensibility limit of roughly 0.1 $C.m^{-3}$ in case of PEA measurements.

1.2	Injection barrier for holes (eV)
5e45	N' for holes $(m^{-3}.J^{-1})$
2000	To for holes (K)
0.81	Δmax for holes (eV)
5e-1	Holes initial density $(C.m^{-3})$
1.1	Injection barrier for electrons (eV)
5e44	N' for electrons $(m^{-3}.J^{-1})$
1200	To for electrons (K)
0.83	Δmax for electrons (eV)
5e-1	Electrons initial density $(C.m^{-3})$
2.3	Relative permittivity
370	Temperature (K)
40e6	Field (V/m)
500e-6	Thickness (m)
500000	Charging time (s)
500000	Decharging time (s)
10	Grid size ratio
301	Cell number
0.05	Gaussian filter factor

Figure 4: Example of parameters text file

When running, a window of the form of that shown in Figure 5 appears. The program can be stopped at any time. The running time for a given cycle depends on the duration of the polarization/depolarization steps, on the velocity of carriers (the time step becomes shorter when this is high, and hence the computation time increases), and on the machine on which it runs. For 3h/3h cycle this can give typically 10min of computation, but it can be also much more (days).
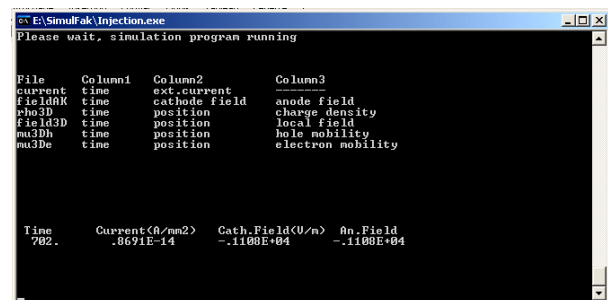

Figure 5: The windows of Injection appearing when simulation is running.

Output data are stored in a set of 8 text files, as detailed in Table 1. 3D files are made of 3 columns, containing respectively time (in s.), position (in m), and the quantity. An exact calculation of the field at the both interfaces is provided in one of these output text files. Of course, the time dependence of the external current, which is one of the variables accessible experimentally, is produced by the model. At this stage, we have not incorporated contributions that could arise from orientation polarization, which would require an expression for the time dependence of the permittivity.

File	Content	Format
rho3D.dat	Net charge density vs. position and time	3D – 3columns
rdh3D.dat	Hole charge density vs. position and time	3D – 3columns
rde3D.dat	Electron charge density vs. position and time	3D – 3columns
mu3Dh.dat	Hole mobility vs. position and time	3D – 3columns
mu3De.dat	Electron mobility vs. position and time	3D – 3columns
field3D.dat	Field vs. position and time	3D – 3columns
fieldAK.dat	Anode and Cathode field vs. time	2D – 3columns
current.dat	Total current vs. time	2D – 2columns

Table 1: Output files produced by Injection

Figure 6 and Figure 7 show an example of output data obtained by this graphic interface. For a better understanding, the curve are plotted in 2D. They correspond respectively to field and space charge density profiles obtained after 1h and 3h under polarization, and 0.5h under short circuit. Note that in this example, the Gaussian filter is has not been applied to the sampece charge density profiles.
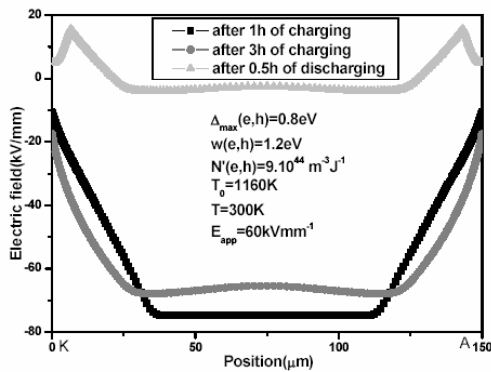

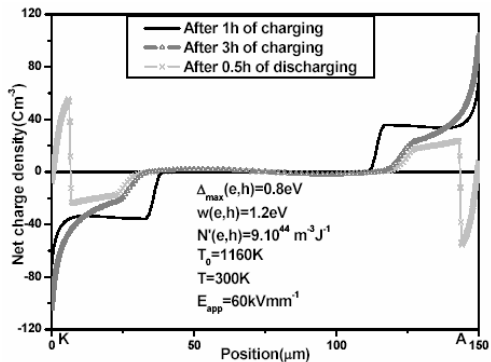**Figure 6: Electric field profiles at different times**

Figure 7: Net charge density taken at three different times 0.5h, 3h of charging, and 0.5h of discharging.

The Interface program

Running simulations

The parameters associated to a given simulation, the list of which being given in Table 4, are dispatched in a set of 3 windows resorting to:
  -Physical parameters of the material and interfaces;
  -Experimental conditions (fields, time, temperature…);
  -Numeric parameters.

Concerning the later, the cell number, i.e. the number of points along the thickness is not an adjustable: it is fixed to 301 in Injection. The grid size ratio defines the ratio of the width of the cell in the middle of the dielectric to that of the cells adjacent to the electrodes (cells are tightened close to the electrodes to improve resolution). Finally, the Gaussian filter factor defines the width of the filter to be used for post-treatment of the data. They are adapted considering experimental profiles (a calibration profile for example).

The Interface program calls the Injection program for running a simulation, making the later transparent to the user.

Exploiting results

Results from simulation being in progress can be visualised while the program Injection is still running. Within a given set of parameters, a number of them are used by Interface to proceed to post-treatment of data. This procedure has a sense only for space charge profiles (especially net space charge). It consists in adding influence charge (capacitive and image charge) and applying the Gaussian filter. Hence, the visualization of a given output file goes with the selection of the relevant parameter text file. Once a data file has been selected, and prior to visualization, one needs to specify the format of the file (and hence of the plot): 2D or 3D, and if the post-treatment –addition of influence charge and filtering – must be done.

An example of 3D plot of field vs. time and thickness is shown in Figure 8. Note that no units are provided so that the tool is very general (3D plots of mobility can be visualized the same way).
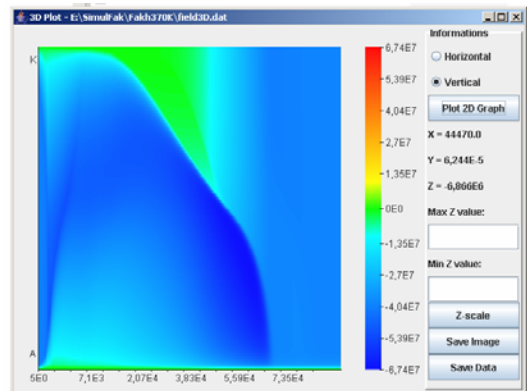

Figure 8: 3D plot of field vs. time and depth and side menu. X-axis corresponds to time in a non-linear scale; Y-axis is the position in the insulation (anode to the bottom, cathode to the top) and colors represent the quantity being plotted with scale given in the color bar.

Simulated data are in a non-linear scale in time. This has been set so to conform to experimental measurements carried out in the project in which the frequency of space charge profiles acquisition is higher just after polarization and depolarization. Hence images themselves are in non-linear scales. The interface can be used to visualize any 3-D pictures and to extract 2-D curves such as profiles at a given time or even to look at the evolution in time of the charge density for a given position.

Finally, Figure 9 shows examples of jpeg images obtained with the 3D plot tool, before and after post-treatment of the data. These results were obtained for 40kV/mm, at 370K and have been produced for a matter of illustration only. However, we can see a charge packet which is made up of injected charges. These ones move across the sample. In experiments, this kind of charge packets can be repeated only a few times, and the magnitude of packet decrease fast during the packet movement.
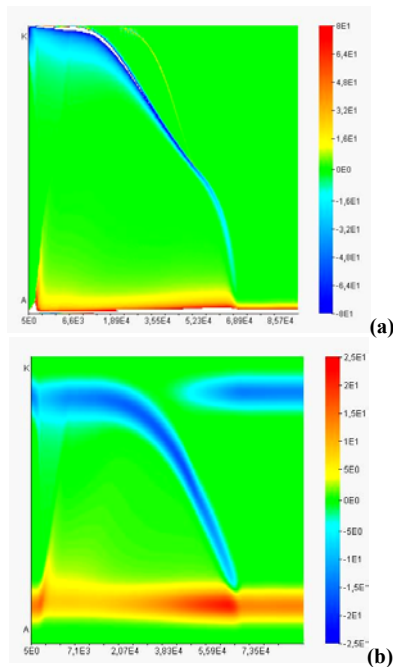

Figure 9: Example of output space charge patterns.
(a): net internal charge produced by the code;
(b): after addition of influence charges and filtering.
Field was on for the whole period of time

CONCLUSION

We have introduced a version of a simulation model designed for describing charge transport in a 1D geometry and plaque samples. It is based on physical grounds that have been shortly recalled. Through this interface, it is possible to input simulation variables (temperature, stress cycle, geometry and intrinsic features of the sample for both kind of carriers…), to run the module for transport in a transparent way, and finally to visualise and handle simulation results, with the possibility to achieve a post-treatment to space charge profile in a form directly comparable to experimental results resorting to the pulsed electro-acoustic method. The tool, which is still in a stage of consolidation as regards its ability to approach the behaviour of different kinds of polyethylene, does lead to progress in

the understanding of dielectric physics in the sense that various hypotheses for explaining a given experimental observation can be evaluated. A comparison between simulation and experimental results is discussed in this conference a companion contribution [9].

Acknowledgments

REFERENCES

[1] J.M. Alison and R.M. Hill, 1994, "*A model for bipolar charge transport, trapping and recombination in degassed crosslinked polyethylene*" *J. Phys. D : Appl. Phys.*, vol. 27, pp. 1291-1299

[2] M. Fukuma, M. Nagao and M. Kosaki, 1994, "*Computer Analysis on Transient Space Charge Distribution in Polymer*", *proc. International Conference on Properties and Applications of Dielectric Materials,* Brisbane (Australia), pp. 24-27.

[3] K. Kaneko, T. Mizutani and Y. Suzuoki, 1999, "*Computer simulation on formation of space charge packets in XLPE films*", *IEEE Trans. Dielectr. Electr. Insul.*, Vol. 6, pp. 152-158.

[4] S. Le Roy, G. Teyssèdre, C. Laurent, G.C. Montanari and F. Palmieri, 2006, "*Description of charge transport in polyethylene using a fluid model with a constant mobility: fitting model and experiments*", *J. Phys. D: Appl. Phys.*, Vol. 39, pp. 1427-1436.

[5] F. Boufayed, G. Teyssèdre, C. Laurent, S. Le Roy, L.A. Dissado, P. Segur, G.C. Montanari, 2006, "*Models of bipolar transport in polyethylene*", *J. Appl. Phys.*, Vol. 100, pp. 104105-104115.

[6] N. Barbey, G. Teyssèdre, 2005, "*Création d'une interface graphique pour un modèle d'étude de charge d'espace*", Rapport de Stage, LGET, 30p.

[7] B.P. Leonard, 1991, *"The ULTIMATE Conservative Difference Scheme Applied to Unsteady One-Dimensional Advection"*, Computer methods in applied mechanics and engineering, Vol. 88, p.17-74

[8] S. Le Roy, G. Teyssèdre and C. Laurent, 2006, *"Numerical methods in the simulation of charge transport in solid dielectrics IEEE Trans. Dielectr. Electr. Insul.,* Vol. 13, pp.239-246

[9] S. Le Roy, F. Baudoin, G. Teyssèdre, C. Laurent, L.A. Dissado and G.C. Montanari, 2007, *"Tools for understanding the thermo-electrical behaviour of XLPE insulation in power cables and accessories", to appear in* Proc. 2007 JCable Conference.